Journal of CO_2 Utilization 19 (2017) 266–275

Contents lists available at ScienceDirect

Journal of CO_2 Utilization

journal homepage: www.elsevier.com/locate/jcou

Adsorption and separation of CO_2 from N_2-rich gas on zeolites: Na-X faujasite vs Na-mordenite

Aline Villarreal[a], Gabriella Garbarino[b], Paola Riani[c], Elisabetta Finocchio[b], Barbara Bosio[b], Jorge Ramírez[a], Guido Busca[b,*]

[a] UNICAT, Departamento de Ingeniería Química, Facultad de Química, Universidad Nacional Autónoma de México (UNAM), Cd. Universitaria, México D.F., Coyoacán 04510, Mexico

[b] DICCA, Department of Civil, Chemical and Environmental Engineering, University of Genoa, Via Montallegro, 1, 16145 Genoa, Italy

[c] DCCI, Department of Chemistry and Industrial Chemistry, University of Genoa, Via Dodecaneso 31, 16146 Genoa, Italy

ARTICLE INFO

Keywords:
Adsorption
Carbon dioxide
Desorption
Faujasite
Mordenite

ABSTRACT

The CO_2 adsorption capacity of Na-MOR and Na-X have been analyzed. The effects of CO_2 concentration, activation temperature, water vapor in the feed, and the desorption/regeneration temperature have been considered. CO_2 adsorption experiments on Na-X and Na-MOR zeolites were made in static conditions with pure CO_2 and in dynamic conditions with N_2/CO_2 mixtures. CO_2 desorption experiments were also made in pure N_2 flow. IR experiments of CO_2 adsorption on dry and wet surfaces were performed. Over both zeolites, when dry, CO_2 is adsorbed reversibly at r.t. in a linear way, as molecular CO_2 interacting with Na^+ ions in a 1:1 or 2:1 CO_2:Na^+ ratio. Over both zeolites, non-linear species also form, i.e. either carbonate-like species or bent CO_2 molecules, or even both. These species are held more strongly and are only desorbed by flowing nitrogen at 373 K. The faujasite zeolite Na-X displays a higher adsorption capacity at high CO_2 partial pressures with respect to Na-MOR, essentially due to the greater amount of active Na^+ ions associated to the lower Si/Al ratio in Na-X. CO_2 adsorption on Na-MOR is strongly diminished when the feed contains 3% water, while on Na-X CO_2 adsorption is slightly enhanced at high P_{CO_2} (60–80%) in wet feed. The IR spectra show that in Na-X CO_2 is absorbed as free hydrogencarbonate ion in water clusters adsorbed into the faujasite cavities. This is not found for Na-MOR.

1. Introduction

Alkali- and alkali earth-containing zeolites, both natural and synthetic, find large industrial application as adsorbents [1,2]. The reversible adsorption of CO_2 on cationic zeolites is a relevant phenomenon, which finds practical application in CO_2 separation technologies. In fact, adsorption techniques are well established and already widely applied commercially to separate CO_2 from hydrogen [3], natural gas [4] and biogas [5–7]. In recent years, the application of similar adsorption techniques to CO_2 capture from flue gases is under study [8]. Adsorption technologies have some advantages with respect to other alternatives (i.e. absorption in amines) such as low cost, applicability to flue gases with variable CO_2 concentration, and environmental friendliness [9–15]. Faujasite zeolite, namely 13X or Na-X, produced commercially and largely applied as an industrial adsorbent, is perhaps the most studied material for CO_2 capture by adsorption. 13X has good performance with several adsorption technologies, i.e. pressure swing adsorption (PSA [16]), vacuum pressure swing adsorption (VSA [17]), temperature swing adsorption (TSA [18]) and electrical swing adsorption (ESA [19]). A number of other zeolites like Na-Y and Cs-Y faujasite [20], zeolites A (Na-LTA or 4A, and Ca-LTA or 5A) [21], Na-ZSM5 [22], and a number of natural zeolites [23] also have acceptable CO_2 adsorption capacities. Relatively few data are reported in the literature for adsorption of CO_2 on mordenite [24], which is another natural zeolite also available commercially in a synthetic form.

Key parameters for the application of zeolites in adsorption of CO_2 from flue gases are the CO_2/N_2 adsorption selectivity, reported to be relatively low on zeolites, as well as the effect of water vapor on the CO_2 adsorption. Most studies report a strong inhibition of CO_2 adsorption by water on Na-X [25,26], which makes necessary a previous drying step for CO_2 capture from flue gases [27]. However, other studies report an efficient CO_2 removal activity by Na-X zeolite in wet gases [28] or even an enhancement of CO_2 adsorption capacity [5]. A positive effect of water pretreatment on the CO_2 adsorption capacity was also found for Cs-Y and Na-Y [20].

In the present study, the behavior of commercial zeolite 13X (Na-X)

* Corresponding author.
E-mail address: Guido.Busca@unige.it (G. Busca).

http://dx.doi.org/10.1016/j.jcou.2017.03.021
Received 7 December 2016; Received in revised form 1 March 2017; Accepted 12 March 2017
Available online 29 April 2017
2212-9820/

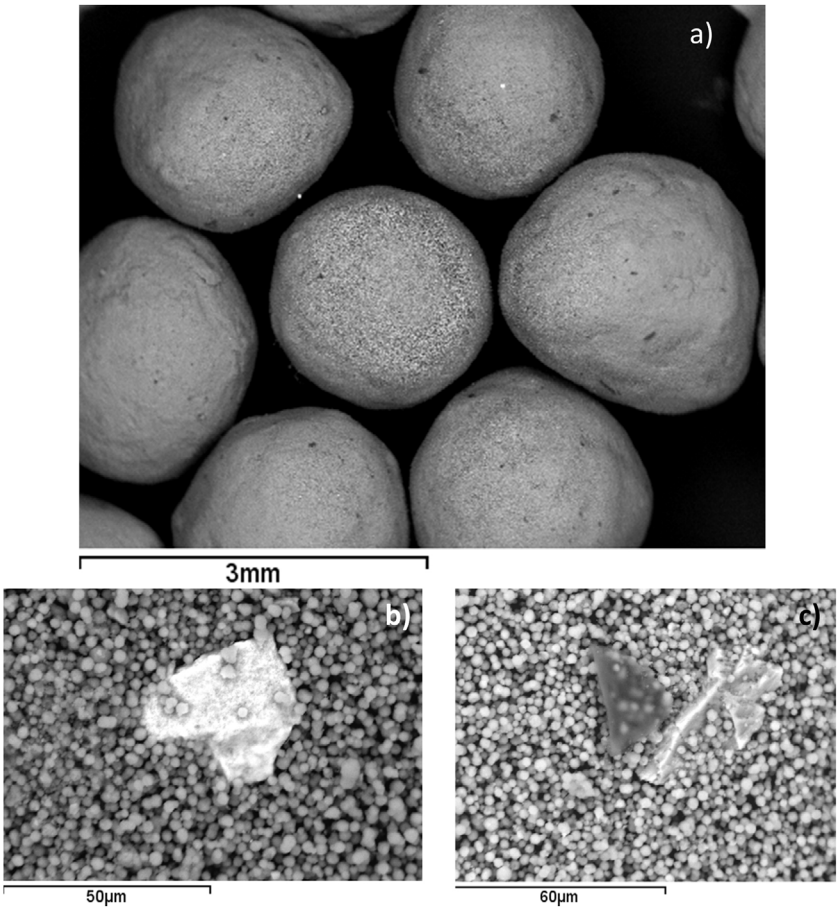

Fig. 1. SEM images of unmilled Na-X beads at different magnifications.

and Na-mordenite (Na-MOR) on the adsorption of CO_2 is compared. The effect of small amounts of water vapor on the CO_2 adsorption capacity of both zeolites, and the nature of the interaction between CO_2 and the adsorption sites in both zeolites was also analyzed.

2. Experimental

Commercial 13X (Na-X) zeolite from Grace, denoted as Sylobead MS C 544 (surface area ~500 m^2/g) was purchased as spherical beads; and used both as beads and, after grinding, as a powder. According to the producer, Na-X contains a small amount of a binder, such as kaolin clay, added to shape the beads [29]. Characterization data on this material have been published elsewhere [5,30,31]. Na-mordenite was a commercial powder from Zeolyst (CBV 10A, SiO_2/Al_2O_3 mole ratio 13, surface area 425 m^2/g). Hereafter the zeolites will be denoted as Na-X and Na-MOR respectively.

Adsorption experiments have been made both in static and in dynamic conditions. For adsorption in static conditions a conventional volumetric apparatus was used, loading 0.4 g of zeolite sieved in the 60–70 mesh range. Prior to the adsorption experiment, the zeolite was activated at 473 K in vacuum for 30 min. Dynamic adsorption tests were performed at room temperature using a tubular quartz reactor (internal diameter of 7 mm), filled with 1.3 g of 60–70 mesh adsorbent material. The adsorbents were exposed to synthetic gas mixtures made from pure gas cylinders from SIAD, as such or saturated in a bubbler with water at room temperature (298 K). Total flow rate was set at 75 NmL/min. Prior to the adsorption experiment, the adsorbent was activated in N_2 flow at 473 K or 573 K for 1 h. According to Thermogravimetric Analysis (TGA) at this temperature water desorption is essentially complete. To analyze the gaseous products, a complete IR spectrum in the mid IR range was taken every 4 s using an on-line FT-IR instrument (ThermoFisher Nicolet 6700), equipped with a gas cell connected to the adsorption apparatus and operating with OMNIC Series acquisition software. This analysis allows monitor the intensity (absorbance) of the diagnostic IR bands for carbon dioxide (an overtone component at 3708 cm^{-1}) and water vapor (1540 cm^{-1}, a rotovibrational component of the H_2O bending mode). The adsorption capacity data have been corrected to cancel the significant delay in the CO_2 concentration detection at the outlet by carrying out separate experiments with a non-adsorbing mass. The estimated experimental error for the adsorption measurement is around 5% and a little higher for experiments in the presence of water.

FT IR spectra of the dry and wet zeolite surfaces were recorded in a FT IR Instrument Nicolet 380 (100 scans, DTGS detector, OMNIC software). Pure powder pressed disks (20 mg average weight) were activated in vacuum at 473, 573 and 673 K in the IR cell ('activated surface') for 1 h, then cooled down to room temperature and contacted with 20–30 Torr of spectroscopically pure CO_2 (from SIO, Milan). The spectra of surface species were recorded in the presence of CO_2 gas at two different partial pressures, after outgassing at room temperature, and after outgassing at 673 K. In co-adsorption experiments, water vapor was admitted to the IR cell until the spectrum did not change, thus the sample was supposed to be saturated by water, either before or after CO_2 adsorption.

The spectra of the activated samples have been subtracted from the spectra obtained after CO_2 contact.

Morphology as well as qualitative and quantitative analyses were carried out by using a scanning electron microscope (SEM) Zeiss Evo 40 equipped with a Pentafet Link Energy Dispersive X-ray Spectroscopy (EDXS) system managed by the INCA Energy software (Oxford Instruments, Analytical Ltd., Bucks, U.K.). For qualitative and quantitative analyses, the samples were analyzed employing an acceleration

voltage of 20 kV, using a Co standard for calibration in order to monitor beam current, gain and resolution of the spectrometer.

3. Results

3.1. SEM/EDX characterization of the materials

The SEM images of the Na-X beads (Fig. 1a) show spheres of the order of 2 mm diameter, which are constituted by particles or aggregates, also quite spherical, whose diameter is of the order of 3 μm (Fig. 1b and c). The SEM image of the powder obtained by grinding the Na-X beads also show particles or aggregates near 2 μm diameter. However, in both cases, some additional much larger (10 μm) and non-spherical particles are found. The EDX analysis of the samples show an overall Si to Al ratio of 1.5 and a Al/Na ratio of 1.1. This composition is roughly that expected for NaX zeolite. However, it is also found the additional presence of Mg, Ca, K, Cl, S, P and Fe (< 1% atomic). On the other hand, analysis performed on the larger non-spherical particles show that they are Si-rich, while also carbon-rich and iron-rich particles are present. This suggests that the binding material can be a silicate mineral species, may be kaolin (whose Si/Al ratio is also ~1) impure of iron oxide, while carbon species may be the result of some organic additive use in the extruding process.

The SEM images of the Na-MOR powder show relatively homogenous particles or aggregates with size of the order of several tens of nm. The EDX analysis shows a Si/Al atomic ratio of roughly 6 and a Na/Al ratio of 1, which approximately corresponds to the virtual composition reported by the producer. The analysis also show the additional presence of traces of titanium.

3.2. CO_2 adsorption isotherms

In Fig. 2, the CO_2 adsorption isotherms on Na-MOR obtained from the static and dynamic experiments are compared. In both experiments the adsorbent bed was activated at 473 K in vacuum and in N_2 flow, respectively. In the static experiments the equilibrium pressures after CO_2 contact were recorded after 1.5 h, when the final pressure did not change during few tens of min. This procedure allows recording the overall isotherm in one working day.

The dynamic experiment was performed using a flow of 75 NmL/min, which corresponds to a space velocity of 3.46 $Nm^3/(h\ kg_{ADS})$, which is well above that applicable to real flue gas [27].

The maximum adsorbed amount of CO_2 measured in static conditions, ~0.13 W_{CO_2}/W_{MOR}, corresponding to 2.9 mol_{CO_2}/kg_{MOR}, is comparable to the value reported by Delgado et al. [24], which is of the order of ~ 3mol_{CO_2}/kg_{MOR}.

The shape of the static and dynamic adsorption isotherms shown in Fig. 3 is similar but the adsorbed amount is always higher for the static

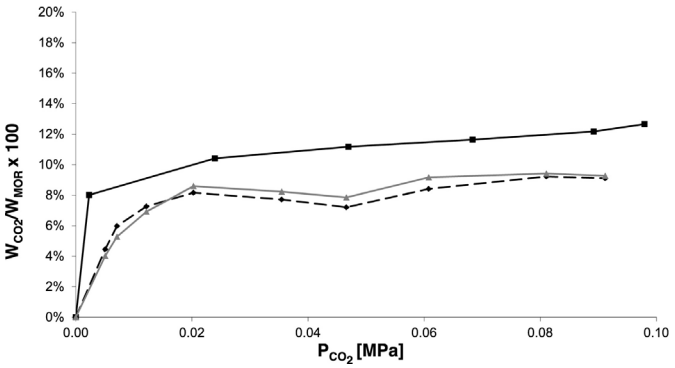

Fig. 2. CO_2 adsorption on Na-MOR activated at 473 K in N_2 atmosphere or vacuum, (♦) dynamic and (■) static experiments and sum of desorbed amount in dynamic experiments (▲). P_{CO_2} is referred to equilibrium pressure in static experiments while for dynamic ones it refers to CO_2 partial pressure.

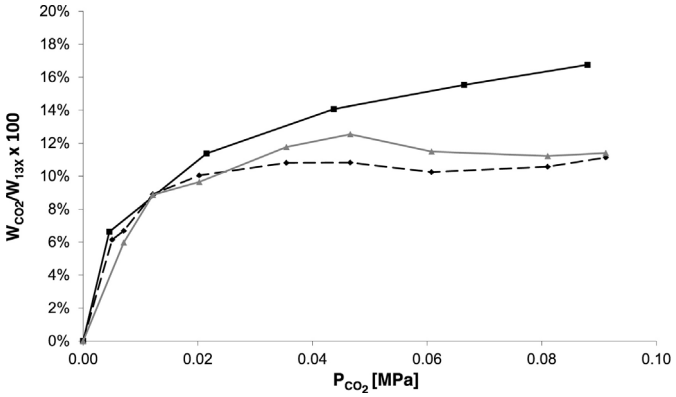

Fig. 3. CO_2 adsorption on Na-X activated at 473 K in N_2 atmosphere or vacuum, (♦) dynamic and (■) static experiments and sum of desorbed amount in dynamic experiments(▲). P_{CO_2} is referred to equilibrium pressure in static experiments while for dynamic ones it refers to CO_2 partial pressure.

experiment, indicating that the data taken in dynamic conditions are either affected by a contribution due to diffusional limitations, or by a competitive adsorption between CO_2 and nitrogen since the static experiment was performed using pure CO_2 whereas the dynamic experiment used mixtures CO_2/N_2. The amounts of the adsorbed species measured in dynamic conditions correspond well with the total amounts of desorbed species at room temperature and at 373 K.

The corresponding curves for Na-X faujasite are reported in Fig. 2. In the low-pressure range the dynamic and static isotherms are very near to each other, while at higher CO_2 pressure the curve recorded in static conditions is far higher than the one recorded in dynamic conditions. This provides evidence of a different behavior with respect to Na-MOR. On Na-X, it is quite evident that a plateau is actually still not reached in static conditions even at P_{CO_2} 0.09 MPa. This different behavior can also be observed looking at the data reported by Choudary et al. [32]. For Na-X, the maximum adsorbed amount observed in static conditions (3.9$mol_{CO_2}/kgNa - X$) is slightly lower than those reported in the literature [5,28,33–38], which are of the order of ~ 4 – 4.5$mol_{CO_2}/kgNa - x$. Thus, the total CO_2 adsorbed on Na-X is higher than on Na-MOR at higher P_{CO_2}, while is similar on the two adsorbents at low P_{CO_2}.

The desorption behavior for Na-MOR and Na-X activated at 473 K is compared in Fig. 4. While most of CO_2 is desorbed by flowing pure nitrogen at r.t., a small amount needs heating to be removed. This amount is slightly higher for Na-MOR than for Na-X, in particular in the low P_{CO_2} range. In contrast, the amount of CO_2 desorbed at r.t. is definitely higher on Na-X than on Na-MOR, but only when the CO_2 content in the feed is more than 20%.

Fig. 5 compares the desorption behavior of the two zeolites after activation at higher temperature (573 K). In general, the sum of the desorbed CO_2 at room temperature and at 373 K was similar to the total CO_2 adsorbed. By increasing the activation temperature, the amount of desorbed (and adsorbed) CO_2 increased more on Na-MOR than on Na-X. Additionally, for Na-MOR the amount of strongly adsorbed CO_2, needing heating at 373 K for desorption, increased significantly, becoming much larger than for Na-X.

The desorption behavior of the two zeolites after activation at 573 K, using a wet feed with 3 vol.% water is compared in Fig. 6. In both zeolites the amount of adsorbed CO_2 is lower in wet than in dry conditions. In particular, the amount of strongly adsorbed CO_2, desorbed only at high temperature, is also strongly reduced in the presence of water. Interestingly, on Na-X the amount of adsorbed CO_2 increases slightly at high CO_2 pressure (e.g. P_{CO_2} ~ 0.06–0.08 MPa).

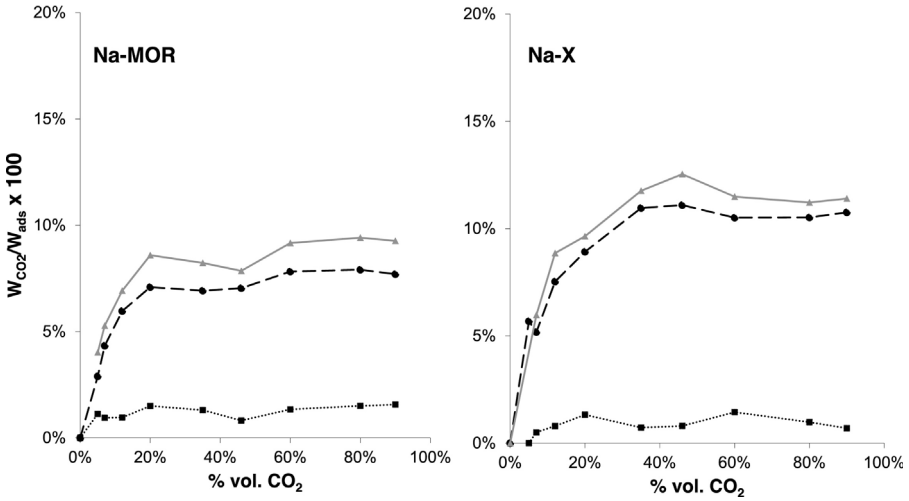

Fig. 4. CO_2 desorption at room temperature (dashed line), desorption at 373 K (dotted line) and sum of desorption (grey line) on Na-MOR and Na-X activated at 473 K.

3.3. FT IR studies

In Fig. 7A, spectra of Na-MOR and Na-X pure powders are reported in the OH stretching spectral region after activation at 573 K. Similar spectra were recorded after activation at 473 and 673 K (not shown). The essential absence of well-defined bands points to the full cationic exchange of both materials, with no hydroxylation except the very small feature at ca. 3735 cm^{-1}, due to few external silanols, in the case of Na-MOR. The spectra of the activated samples in the lower frequency side are reported in Fig. 7B. In the case of Na-MOR the broad bands observed in the low frequency region are due to overtones of the bulk modes. The cut-off limit due to the bulk Si–O–T (T = Al or Si) asymmetric stretching modes is found definitely higher for Na-MOR than for Na-X, due to the higher position of the fundamental mode, associated to its higher Si/Al atomic ratio. No bands with significant intensity due to adsorbed species are observed after activation at 573 K, suggesting that at these temperatures both surfaces are essentially clean. Only in the case of Na-MOR activated at 473 K a weak additional doublet is found at ca 1650 and 1615 cm^{-1}, which disappears by outgassing at higher temperatures.

CO_2 adsorption spectra were recorded: (i) in the presence of CO_2; (ii) after outgassing at room temperature; and (iii) after outgassing at increasing temperature up to the activation temperature (Fig. 8). At high CO_2 pressure, in the spectra of Na-MOR treated at 473 K, the signal due to CO_2 asymmetric stretching vibrational mode is very strong, raising saturation, with a weaker band at 2293 cm^{-1} due to naturally occurring isotopic $^{13}CO_2$ (Fig. 8A). After outgassing, therefore at lower surface coverage, the maximum of the main band of physisorbed CO_2 shifts to 2360 cm^{-1} possibly showing a shoulder at 2350 cm^{-1}. This suggests that two different linear species can be formed, maybe a 1:1 and a 2:1 CO_2: Na complex, as discussed by Bonelli et al. [39]. By increasing the activation temperature to 573 K and 673 K, an increased relative intensity of this band, which also appears slightly shifted toward higher frequencies, is observed after outgassing. The position of this band, always centered at higher frequency than in gaseous CO_2, points out the coordination of CO_2 at surface Na^+ Lewis sites through the O atoms, indicating therefore a linear structure [5].

In the low frequency region, above the cut off of the zeolite network, a triplet of bands with maxima at 1691–88, 1638–33, 1612–11 cm^{-1}, resisting outgassing and assigned to the products of CO_2 chemisorption. Another weaker band is also detected near 1380 cm^{-1}. The bands in the region 1700–1600 cm^{-1} are similar to those already present in the sample activated at 473 K. These bands, similar to those attributed to bridging or bidentate carbonate species on different surfaces [40] including Na zeolites [41,42], are due to the higher frequency component of the split asymmetric stretching mode of the carbonate ion. The lower frequency counterpart of the split asymmetric stretching mode is likely masked by the skeletal modes falling below the cut-off limit. An alternative possibility is to assign the observed bands to strongly perturbed bent CO_2 molecules [43]. The weak band at 1380 cm^{-1} is due to the symmetric stretching mode of the linearly adsorbed CO_2 molecules, which is IR inactive and Raman active at 1388 cm^{-1} in the gas, but can be weakly activated in the adsorbed state due to the lowering of the molecule symmetry.

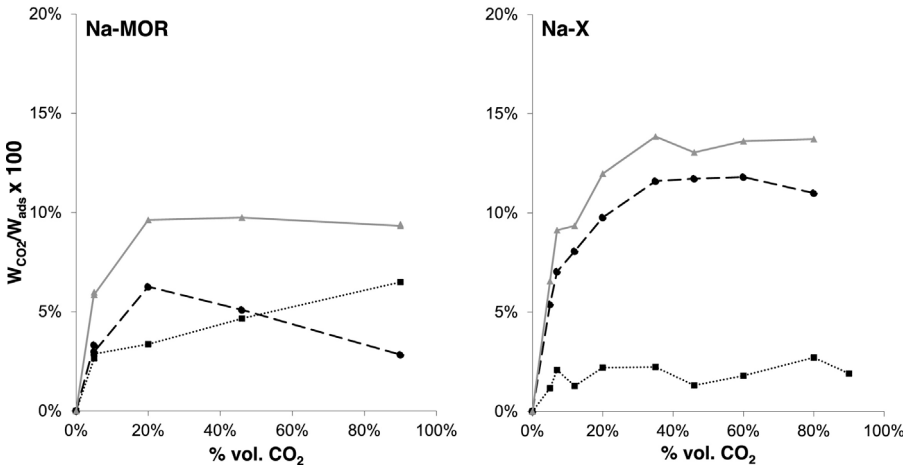

Fig. 5. Desorption at room temperature (dashed line), desorption at 473 K (dotted line) and sum of desorption (grey line) on Na-MOR and Na-X activated at 573 K.

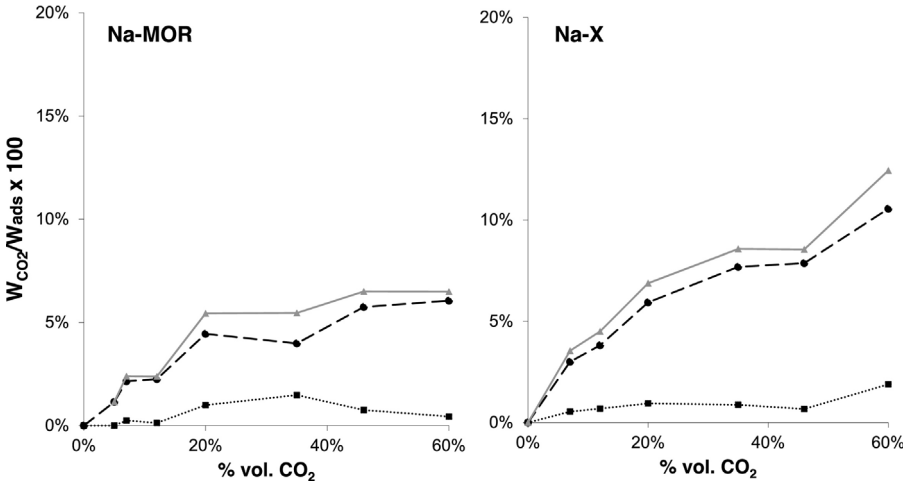

Fig. 6. Results of CO_2 adsorption in presence of water, desorption at room temperature (dashed line), desorption at 473 K (dotted line) and sum of desorption on Na-MOR and Na-X activated at 573 K (% vol. CO_2 on dry basis).

Bands in the 1690–1610 cm^{-1} region increase upon outgassing while molecularly adsorbed CO_2 disappears, suggesting that when linear CO_2 molecules desorb, more space is obtained for CO_2 molecules to bridge over oxide species. These bridged species are still detected after outgassing up to 473 K (Fig. 8A), in agreement with the observation of these bands in the sample activated at 473 K. This explains the fraction of CO_2 that is desorbed only by heating above room temperature after the dynamic adsorption experiments. After outgassing at 573 K and 673 K, no more adsorbed species can be observed (Fig. 8B and C, respectively).

The comparison between the spectra reported in Fig. 8A–C shows that the same features are detected on Na-MOR at the different activation temperatures. Activation of the surface at 573–673 K seems to slightly reduce the overall band intensity of chemisorbed species while increasing the resistance to outgassing of molecularly adsorbed CO_2.

In another set of experiments, the Na-MOR zeolite previously activated at 673 K (Fig. 9a) was saturated at room temperature with water vapor and briefly outgassed at r.t. (Fig. 9b), thus obtaining a wet surface before CO_2 adsorption. The very strong band centered at 1626 cm^{-1} with an additional component near 1642 cm^{-1} is assigned to water scissoring vibration mode, the corresponding OH stretching being responsible for the very strong absorption in the region 3700–3000 cm^{-1}. CO_2 adsorption over this wet surface gives rise (Figs. 9c and 10 , top) to a main band at 2345 cm^{-1}, sharp and almost symmetric and readily disappearing after outgassing. Difficult to say whether the band triplet previously assigned to “non-linear” species formed on the dry surface is present, being superimposed to the scissoring mode of adsorbed water (Fig. 8, spectra b–c and Fig. 10, bottom). Indeed, the modifications undergone by the spectrum of adsorbed water appear more as due to a slight perturbation of the state of adsorbed water than as due to the superimposition of other bands. Thus, only a very weak molecular adsorption seems to occur on the wet Na-MOR surface, likely due to CO_2 molecules weakly hydrogen bonded with water molecules.

The IR spectra of CO_2 adsorption over Na-X after activation at 473 K, 573 K and 673 K is shown in Fig. 11. The strong band with maximum at 2340 cm^{-1} is assigned to CO_2 physisorbed (OCO asymmetric stretching) almost not perturbed. Shoulders at 2350 and 2370 cm^{-1} can be assigned to CO_2 coordinated through oxygen atoms to Na^+ Lewis sites. Correspondingly, in the low frequency region of the spectrum, several sharp bands are detected at 1706, 1645, 1610, 1481, 1423, 1360 cm^{-1}, all of them assigned to chemisorbed non-linear species, as reported previously for CO_2 adsorption over the same material after activation at higher temperature [6,25,44]. The multiplicity of bands in the 1700–1600 cm^{-1} spectral region, as well as the bands at 1486 and 1428 cm^{-1} suggest the existence of a mixture of carbonate-like species, likely both monodentate, and bidentate or bridging. The possibility of assigning these bands, at least in part, to bent CO_2 molecules cannot be excluded. The different activation temperatures (473, 573, 673 K, as reported in Fig. 11A–C, respectively) do not affect significantly the nature of surface adsorbed species.

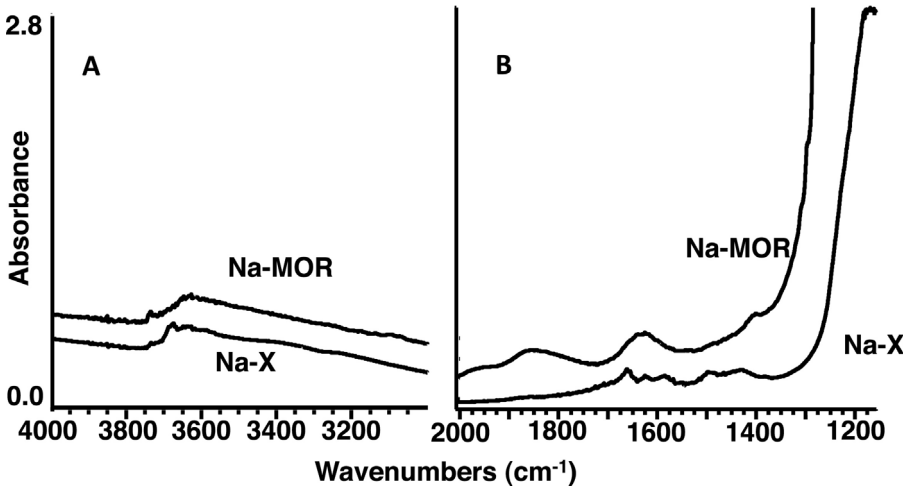

Fig. 7. FT IR spectra of Na-MOR and Na-X zeolite activated at 573 K.

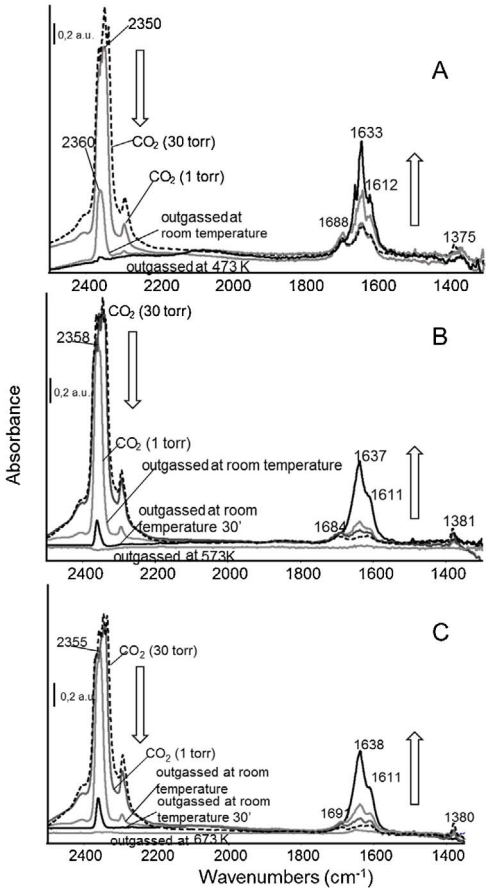

Fig. 8. FT IR subtraction spectra of surface species arising from CO_2 adsorption over Na-MOR, after activation of the sample at 473 K (A), 573 K (B), 673 K (C).

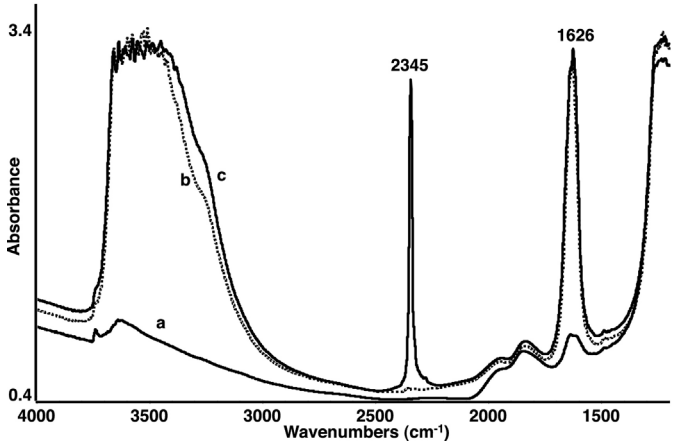

Fig. 9. FT IR spectra of the Na-MOR sample after activation at 473 K (a), saturation with water vapor and further outgassing at r.t. (b), successive contact with CO_2 gas (c).

Fig. 12, displays the spectra of the Na-X zeolite previously saturated by water, before and after CO_2 adsorption. In contact with CO_2 the OCO stretching of linear CO_2 is well evident, centered at 2345 cm^{-1}, quite symmetric. Upon outgassing this band quickly disappears. An additional quite strong band appears at 1360 cm^{-1}, together with an evident shoulder near 1405 cm^{-1}. The result is closely similar to that reported previously for a similar experiment [6].

As discussed previously, the bands in the region 1400–1360 cm^{-1} correspond quite well with the two peaks observed in the Raman spectrum of aqueous hydrogencarbonate ion [45]. These features slowly disappear by outgassing at r.t. (Fig. 13). These data strongly suggest that carbon dioxide absorbs on the wet Na-X surface mainly in

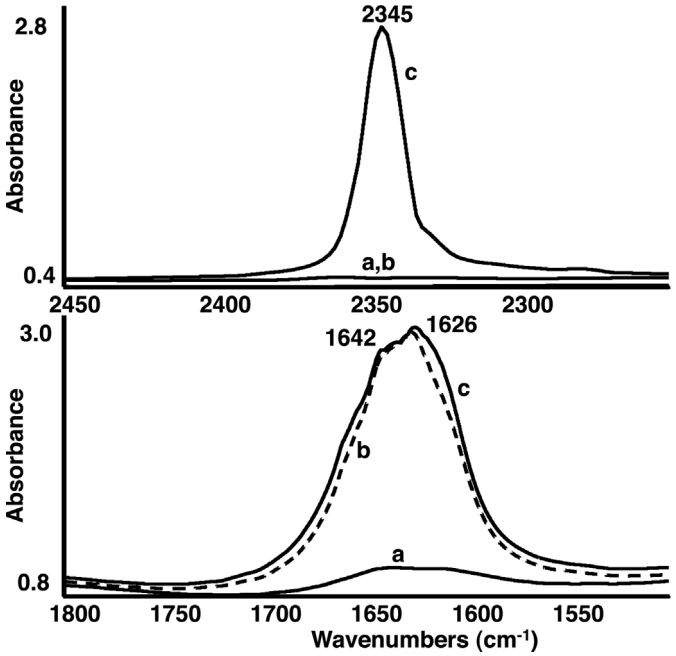

Fig. 10. FT IR spectra of surface species after CO_2 adsorption on wet Na-MOR (a), saturation with water vapour and further outgassing at r.t. (b), successive contact with CO_2 gas (c).

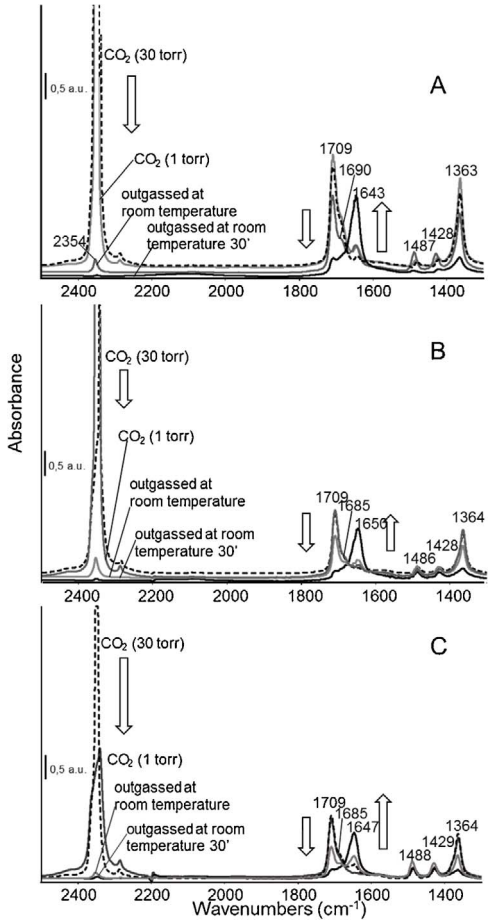

Fig. 11. FT IR subtraction spectra of surface species arising from CO_2 adsorption over Na-X after activation of the sample at 473 K (A), 573 K (B), 673 K (C).

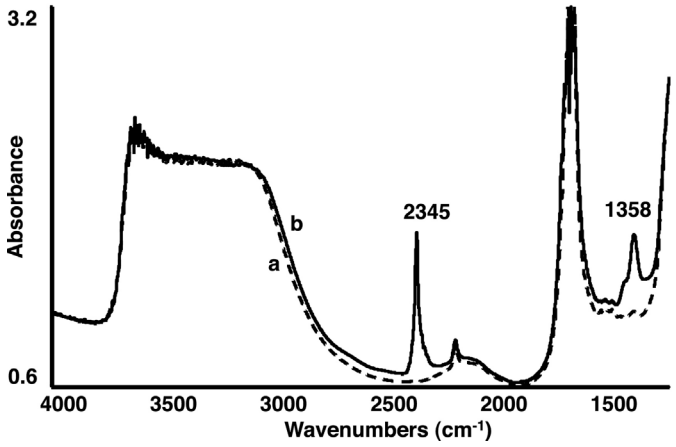

Fig. 12. FT IR spectra of the Na-X sample after activation at 473 K, (a) saturation with water vapor and further outgassing at r.t., (b) successive contact with CO_2 gas.

the form of hydrogencarbonate ion on or in adsorbed water in the faujasite cavities. The reactive absorption is likely the typical one for CO_2 absorption in water:

$$CO_2 + H_2O \leftrightarrows HCO_3^- + H^+$$

4. Discussion

The data described above show that both Na-MOR and Na-X zeolites are active in the reversible adsorption of CO_2 from N_2/CO_2 mixtures in ambient conditions. However, the total CO_2 adsorbed on NaX is higher than on Na-MOR at higher P_{CO_2}, while is similar on the at low P_{CO_2}.

Experiments performed in static conditions with pure CO_2 give rise to higher adsorbed amounts than those recorded in dynamic conditions using CO_2/N_2 mixtures, suggesting that in dynamic conditions either diffusion limitation phenomena are present on both adsorbents or that competitive adsorption between CO_2 and N_2 could be not negligible.

On both Na-X and Na-MOR, most of the adsorbed CO_2 is reversibly desorbed by simple purging with pure nitrogen at room temperature although a fraction of strongly adsorbed CO_2 (10–30%) needs heating for desorption. The fraction of strongly adsorbed CO_2 is higher on Na-MOR than on Na-X and increased significantly, from 10% to 30%, when the Na-MOR sample was activated at 573 K.

The results of the adsorption of CO_2 followed by IR and the analysis of the structure of the two zeolites can help to obtain valuable information concerning the real mechanism of adsorption of CO_2 on Na-zeolites. Previous theoretical and experimental investigations strongly support the idea that the interaction of CO_2 is mainly associated to Lewis acid-base type O-bonding of CO_2 with sodium cations. Interestingly, however, a number of different possibilities have been considered for the "geometry" as well as for the structure of this interaction. The interaction can occur with a single Na^+ ion to which one [46] or two [39] CO_2 molecules bond, by interaction with one M^+ cation and the nearest oxygen anions still retaining linearity [41], with two cations (one oxygen each), still retaining linearity [47], or even with three cations [48]. Additionally, formation of carbonate-like species with the participation of framework oxygen atoms has also been reported [49], while the possible formation of adsorbed bent CO_2 molecules, commonly occurring for species interacting with transition metal ions [50], can also be possible upon adsorption on Lewis acid sites [43].

Our data show that in the case of both Na-MOR and Na-X when dry, CO_2 adsorption occurs both in the form of linear CO_2 species O-bonded over Na^+ ions and as non-linear ones. In fact, the adsorbed CO_2 species responsible for the strong band centered at 2365–2340 cm^{-1}, due to the OCO asymmetric stretching mode, are certainly linear, while those responsible for bands in the 1700–1380 cm^{-1} are positively not linear. It is clear from the data that the non-linear species are adsorbed more strongly than the linear ones. Indeed, the data show that most of the reversible adsorption and desorption of CO_2 occurring at room temperature on both zeolites involves the linear species. However, non-linear species certainly compete with the linear ones for the interaction with Na^+ ions and might also inhibit them, being stronger. At high coverage, linear coordinated molecular species predominate but upon outgassing, part of them converts into carbonate-like species, suggesting that some of the two species interact with the same Na^+ cations. The presence of non-linear species must be taken into account in particular for Temperature Swing Adsorption applications, when desorption upon heating could occur in two steps.

The ideal faujasite structure consists of wide supercages (13 Å diameter) accessed through 12-member silicate rings with 7.4 Å diameter, much smaller sodalite cages accessed through 6-member silicate rings and hexagonal prisms connecting the sodalite cages. Exchanged Na^+ cations sit on different sites called site I (with the alternative of site I′), site II, and site III (with the alternatives of site III′a and III′b [51–53]). Site I is in the center of the hexagonal prism (16 per unit cell) while the alternative sites I′ are just over the 6MR in the sodalite cage (32 per unit cell). Site II (32 per unit cell) is just above the center of the 6MR separating supercages and sodalite cages. Site III (48 per unit cell) is just above the 4MR separating supercages and sodalite cages, but has alternatives in sites III′, III′a and III′b, in near positions off center the 4MR [51].

A theoretical perfect low silica Na-X (Na-LSX, with Si/Al = 1) has full occupation of sites I and II, and essentially half occupation of sites III, with no occupation of sites I′, III′a and III′b. In the case of the Na-X zeolite (like the one used here), with Si/Al ratio 1.2–2, occupancy of sites I is < 1, with some occupancy of sites I′, occupation of site II is still

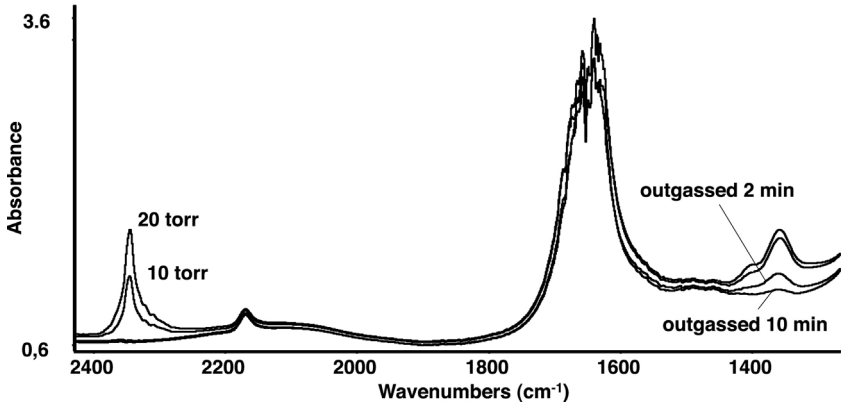

Fig. 13. FT IR spectra of the Na-X sample after activation at 473 K, saturation with water vapor and further outgassing at r.t., successive contact with CO_2 gas 20 Torr, and progressive outgassing at 10 Torr, and 0 Torr 2 min and 10 min.

essentially full, while occupancy of sites III is low, the alternative sites III′a and III′b being mainly occupied. Due to the small size of the windows, it is supposed that sodalite cages and hexagonal prisms, where sites I and I′ are located, are inaccessible to polyatomic molecules. Thus, the entire adsorption chemistry of faujasites would occur in the supercages, and involves only the ions located there. These large cavities contain (for the Na-X structure) in average a little less than 10 Na^+ ions, 4 of which are located at site II and a little less than 6 located in sites III′a and III′b. These Na^+ ions have very low overall coordination with quite weak coordination bonds, and may also be influenced by their mutual electrostatic repulsion. This explains their significant Lewis acidity, and their ability to interact with more than one CO_2 molecule, both in the linear molecular way and as a bent molecule or a carbonate species. Taking into consideration these data, it is possible to calculate that 5.87 mol of "active" Na ions are present per kg of dry ideal and binder-free Na-LSX zeolite. The measured value of the total adsorbed amount of CO_2 on Na-X (4.5 mol/kg_{NaX}) appears to be in good agreement indicating a near 1:1 average ratio between adsorbed CO_2 and Na^+ ions on NaX. However, as remarked above, the curve recorded on Na-X in static conditions does not show a real plateau, but is still raising at the highest CO_2 partial pressures. On the other hand, on Na-X the adsorbed amount measured in static conditions is similar to that measured in dynamic conditions at low P_{CO_2}, while is definitely higher at high P_{CO_2}. These data could be tentatively explained by assuming that adsorption occurs rapidly near the cavity mouths, which are easily occupied at low P_{CO_2}, but is slower in the most internal cavities as an effect of the slow diffusion of CO_2 in the cavities, due to the high density of Na^+ ions and already adsorbed CO_2 molecules. In our experiments performed in static conditions, the contact time seems sufficient for the occupation of the internal sites of Na-X at high P_{CO_2}.

The orthorhombic mordenite structure [54] is characterized by nearly straight "main" channels running along the [001] crystallographic direction, which are accessible through 12-membered (elliptical) silicon-oxygen rings having 6.5 Å × 7.0 Å diameters. Additionally, 8-ring "side pockets" exist in the [010] direction having 3.4 Å × 4.8 Å diameter, which however do not allow flow of molecules being in fact interrupted by narrow-necked obstructions. The side pockets connect the 12 ring main channel to a distorted eight-ring compressed channel also running parallel to the [001] direction, but having an elliptical compressed opening 5.7 Å × 2.6 Å wide. The localization of Na^+ in Na-MOR samples has been the object of several studies [55–57]. Assuming the idealized composition for dehydrated MOR $Na_8Si_{40}Al_8O_{96}$ (Si/Al = 5) it seems quite established that half of the Na^+ ions are located just in the middle of the small compressed channels in the site called (I) or A. It is usually supposed that only monoatomic species can enter the smaller channels of Na-MOR, therefore they would not be available for CO_2. The other half Na^+ ions are distributed between site IV, also called D, near the opening of the side pocket in the main channel, and in position VI, also called E, which is well exposed in the main channel. Both D and E sites should be active in CO_2 adsorption. Thus for a mordenite with Si/Al = 5, we calculate 1.3 mol of active Na per kg. The lower amount of active sodium ions justifies the lower adsorption capacity of Na-MOR with respect to Na-X, but also suggests that in the Na-MOR the CO_2: Na_{ACT} is near 2, with a large contribution of double coordination (two CO_2 molecules per one Na^+ ion).

As discussed above, the static isotherm on Na-MOR apparently is asymptotic, in contrast to that observed on Na-X which is not. This is possibly associated to the smaller density of Na^+ ions and adsorbed CO_2 in the straight channels of MOR than in the cavities of faujasite, allowing faster diffusion toward the internal sites also at relatively low P_{CO_2}. On the other hand, the amount of CO_2 adsorbed on Na-MOR in dynamic conditions (with N_2/CO_2 feed) is definitely lower than that adsorbed in static conditions (performed with pure CO_2) for all the CO_2 partial pressures used here. This suggests the presence of diffusion limitation effects in our measures in dynamic conditions or some competition of CO_2 and N_2 adsorption, more relevant for Na-MOR than for Na-X. On the other hand, it has been reported than Na-X zeolite has a higher selectivity for CO_2 adsorption with respect to N_2 adsorption than Na-MOR (Si/Al near 6) [14]. The effect of the presence of N_2 on the adsorption of CO_2 on Na-X was the object of a recent study, where this effect was shown to be small but non-completely negligible at low CO_2 pressures and high N_2 pressures [58]. According to the literature, on both Na-X and Na-MOR the amount of adsorbed N_2 is much lower than the amount of adsorbed CO_2 [14,59]. Also, the amounts of N_2 adsorbed on Na-X and Na-MOR are similar. In the case of our Na-MOR sample, we measured the adsorption isotherm of N_2 in static conditions, and found a very small adsorption at low pressures but up to W_{N_2}/W_{NaMOR} 3% wt./wt. at 0.085 MPa, which indeed confirms that the adsorption of CO_2 on Na-MOR at low P_{CO_2} can be affected by the presence of N_2.

The bigger amount of strongly adsorbed CO_2 on Na-MOR, in particular after activation at higher temperature, could be associated to the presence of more active sites for adsorption of both CO_2 (in the form of non-linear species) on the dry surfaces, and water. These sites may be tentatively identified as Na^+ ions interacting with the anionic framework located in the side pockets (sites D or IV).

In the experiments performed in dynamic conditions with wet feed, the total amount of water in the feed, was not enough to fully rehydrate the zeolites, and only partially decreased the amount of adsorbed CO_2 in both zeolites at relatively low P_{CO_2}. However, at high CO_2 partial pressure, in the case of Na-X zeolite the presence of water vapor in the feed results in a slight increase of the amount of adsorbed CO_2.

From the IR spectra in the presence of water, it seems that only uncoordinated CO_2 molecules adsorb on the Na-MOR sample, possibly H-bonded on adsorbed water. On Na-X uncoordinated hydrogencarbonate species apparently form, probably due to the reaction of CO_2 with water filling the zeolite cavities. The different behavior of Na-MOR with respect to Na-X, when wet, can be ascribed to the larger cavities of Na-X, allowing the formation of larger adsorbed water clusters (which are more basic than smaller clusters [60]) as well as with the different composition of the framework, likely giving rise to a more basic character of the environment of Na-X with respect to Na-MOR.

5. Conclusions

The data reported and discussed above provide evidence of the properties of Na-X and Na-MOR zeolites for the adsorption of CO_2 from the pure gas or N_2/CO_2 mixtures. Over both zeolites, when dry, CO_2 is reversibly adsorbed at r.t. in a linear way, as molecular CO_2 interacting with Na^+ ions. It seems likely that, on Na-MOR, more than one CO_2 molecule, nearly two in average, adsorb on the same Na^+ ion. Over both zeolites, non-linear species also form, i.e. either carbonate-like species or bent CO_2 molecules, or even both. These species are held strongly and are only desorbed by flowing nitrogen upon heating at 373 K. The amount of strongly adsorbed species increases significantly with the activation temperature in the case of Na-MOR.

Faujasite Na-X zeolite has higher adsorption capacity than Na-MOR at the high CO_2 partial pressures due to the greater amount of active Na^+ ions associated to the lower Si/Al ratio in Na-X compared to Na-MOR. At low CO_2 partial pressure in static conditions, the amount of CO_2 adsorbed on the two zeolites is similar.

Some diffusional limitations or competition between the adsorption of CO_2 and N_2 are probably the cause of the lower adsorption capacity obtained in the dynamic adsorption experiments, especially for Na-MOR.

The presence of water vapor in the feed, strongly reduces the CO_2 adsorption on Na-MOR and Na-X at low P_{CO_2}. Interestingly, at high P_{CO_2} (0.06–0.08 MPa) the adsorption of CO_2 is slightly enhanced only on Na-X. The IR spectra revealed that in the faujasite cavities water clusters form and absorb CO_2 in the form of free hydrogencarbonate ion.

Na-MOR can be used to adsorb CO_2 from low concentrated streams

but a previous dehydration step is necessary for an improved adsorption.

Acknowledgements

Aline Villarreal is grateful to CONACyT for her PhD grant 419865. We are also grateful to the financial support of the Faculty of Chemistry-UNAM through PAIP-5000-9072.

References

[1] S. Sircar, A.L. Myers, Gas separation by zeolites, in: S.M. Auerbach, K.A. Carrado, P.K. Dutta (Eds.), Handbook of Zeolite Science and Technology, CRC Press, 2003, pp. 1063–1104.
[2] G. Busca, Heterogeneous Catalytic Materials, Solid State Chemistry, Surface Chemistry and Catalytic Behaviour, Elsevier Publishing, 2014, pp. 204–212.
[3] Hydrogen Recovery by Pressure Swing Adsorption, Linde, (2015) Brochure Available on Internet: http://www.linde-engineering.com/internet.global.lindeengineering.global/en/images/HA_H_1_1_e_12_150dpi19_6130.pdf (08.10.15).
[4] M. Tagliabue, D. Farrusseng, S. Valencia, S. Aguado, U. Ravon, C. Rizzo, A. Corma, C. Mirodatos, Natural gas treating by selective adsorption: material science and chemical engineering interplay, Chem. Eng. J. 155 (2009) 553–566.
[5] A. Petersson, A. Wellinger, Biogas Upgrading Technologies – Developments and Innovations, IEA Bioenergy, 2009Available on Internet 5.11.2016.
[6] T. Montanari, E. Finocchio, E. Salvatore, G. Garuti, A. Giordano, C. Pistarino, G. Busca, CO_2 separation and landfill biogas upgrading: a comparison of 4A and 13X zeolite adsorbents, Energy 36 (2011) 314–319.
[7] Q. Sun, H. Li, J. Yan, L. Liu, Z. Yu, X. Yu, Selection of appropriate biogas upgrading technology – a review of biogas cleaning, upgrading and utilisation, Renew. Sustain. Energy Rev. 51 (2015) 521–532.
[8] B. Sreenivasulu, I. Sreedhar, P. Suresh, K.V. Raghavan, Development trends in porous adsorbents for carbon capture, Environ. Sci. Technol. 49 (2015) 12641–12661.
[9] M. Songolzadeh, M. Soleimani, M. Takht Ravanchi, R. Songolzadeh, Carbon dioxide separation from flue gases: a technological review emphasizing reduction in greenhouse gas emissions, Sci. World J. (2014) 828131.
[10] D.Y.C. Leung, G. Caramanna, M.M. Maroto-Valer, An overview of current status of carbon dioxide capture and storage technologies, Renew. Sustain. Energy Rev. 39 (2014) 426–443.
[11] Q. Wang, J. Luo, Z. Zhong, A. Borgna, CO_2 capture by solid adsorbents and their applications: current status and new trends, Energy Environ. Sci. 4 (2011) 42–55.
[12] M.M. Lozinska, E. Mangano, J.P.S. Mowat, A.M. Shepherd, R.F. Howe, S.P. Thompson, J.E. Parker, S. Brandani, P.A. Wright, Understanding carbon dioxide adsorption on univalent cation forms of the flexible zeolite RHO at conditions relevant to carbon capture from flue gases, J. Am. Chem. Soc. 134 (2012) 17628–17642.
[13] P.A. Webley, Adsorption technology for CO_2 separation and capture. A perspective, Adsorption 20 (2014) 225–231.
[14] G.D. Pirngruber, V. Carlier, D. Leinekugel-le-Cocq, Post-combustion CO_2 capture by vacuum swing adsorption using zeolites – a feasibility study, Oil Gas Sci. Technol. Rev. IFPEN 69 (2014) 989–1003.
[15] J.A. Arran Gibson, E. Mangano, E. Shiko, A.G. Greenaway, A.V. Gromov, M.M. Lozinska, D. Friedrich, E.E.B. Campbell, P.A. Wright, S. Brandani, Adsorption materials and processes for carbon capture from gas-fired power plants: AMP gas, Ind. Eng. Chem. Res. 55 (2016) 3840–3851.
[16] Y. Takamura, J. Aoki, S. Uchida, S. Narita, Application of high-pressure swing adsorption process for improvement of CO_2 recovery system from flue gas, Can. J. Chem. Eng. 79 (2001) 812–816.
[17] J. Ling, A. Ntiamoah, P. Xiao, D. Xu, P.A. Webley, Y. Zhai, Overview of CO_2 capture from flue gas streams by vacuum pressure swing adsorption technology, Austin J. Chem. Eng. 1 (2014) 1009.
[18] D. Bahamon, L.F. Vega, Systematic evaluation of materials for post-combustion CO_2 capture in a temperature swing adsorption process, Chem. Eng. J. 284 (2016) 438–447.
[19] C.A. Grande, R.P. Ribeiro, A.E. Rodrigueas, Challenges of electric swing adsorption for CO_2 capture, ChemSusChem 3 (2010) 892–898.
[20] E. Dıaz, E. Muñoz, A. Vega, S. Ordoñez, Enhancement of the CO_2 retention capacity of Y zeolites by Na and Cs treatments: effect of adsorption temperature and water treatment, Ind. Eng. Chem. Res. 47 (2008) 412–418.
[21] J. Merel, M. Clausse, F. Meunier, Experimental investigation on CO_2 post-combustion capture by indirect thermal swing adsorption using 13X and 5A zeolites, Ind. Eng. Chem. Res. 47 (2008) 209–215.
[22] S.K. Wirawan, D. Creaser, CO_2 adsorption on silicalite-1 and cation exchanged ZSM-5 zeolites using a step change response method, Micropor. Mesopor. Mater. 91 (2006) 196–205.
[23] R. Hernandez-Huesca, L. Dıaz, G. Aguilar-Armenta, Adsorption equilibria and kinetics of CO_2, CH_4 and N_2 in natural zeolites, Sep. Purif. Technol. 15 (1999) 163.
[24] J.A. Delgado, M.A. Uguina, J.M. Gómez, L. Ortega, Adsorption equilibrium of carbon dioxide, methane and nitrogen onto Na- and H-mordenite at high pressures, Sep. Purif. Technol. 48 (2006) 223–228.
[25] S.U. Rege, R.T. Yang, A novel FTIR method for studying mixed gas adsorption at low concentrations: H_2O and CO_2 on NaX zeolite and γ-alumina, Chem. Eng. Sci. 56 (2001) 3781–3796.
[26] F. Brandani, D.M. Ruthven, The effect of water on the adsorption of CO_2 and C_3H_8 on type X zeolites, Ind. Eng. Chem. Res. 43 (2004) 8339–8344.
[27] Y. Lu Wang, W. Yang, X. Shen, P. Kong, J. Li, A.E. Yu, Rodrigues, Experimental evaluation of adsorption technology for CO_2 capture from flue gas in an existing coal-fired power plant, Chem. Eng. Sci. 101 (2013) 615–619.
[28] G. Li, P. Xiao, P.A. Webley, J. Zhang, R. Singh, Competition of CO_2/H_2O in adsorption based CO_2 capture, Energy Proc. 1 (2009) 1123–1130.
[29] Grace, Synthetic Non Fibrous Zeolites Product Stewardship Summary, Available on Internet.
[30] T. Montanari, E. Finocchio, I. Bozzano, G. Garuti, A. Giordano, C. Pistarino, G. Busca, Purification of landfill biogases from siloxanes by adsorption: a study of silica and 13X zeolite adsorbents on hexamethylcyclotrisiloxane separation, Chem. Eng. J. 165 (2010) 859–863.
[31] T.K. Phung, M.M. Carnasciali, E. Finocchio, G. Busca, Catalytic conversion of ethyl acetate over faujasite zeolites, Appl. Catal. A: Gen. 470 (2014) 72–80.
[32] V.R. Choudary, S. Mayadevi, A.P. Sing, Sorption isotherms of methane, ethane, ethene and carbon dioxide on NaX, NaY and Na-mordenite zeolites, J. Chem. Soc., Faraday Trans. 91 (1995) 2935–2944.
[33] D. Ko, R. Siriwardane, L.T. Biegler, Optimization of a pressure swing adsorption process using zeolite 13X for CO_2 sequestration, Ind. Eng. Chem. Res. 42 (2003) 339–348.
[34] S.U. Rege, R.T. Yang, M.A. Bozanowskil, Sorbents for air prepurification in air separation, Chem. Eng. Sci. 55 (2000) 4827–4838.
[35] Z.M. Wang, T. Arai, M. Kumagai, Adsorption separation of low concentrations of CO_2 and NO_2 by synthetic zeolites, Energy Fuels 12 (1998) 1055–1060.
[36] S. Cavenati, C.A. Grande, A.E. Rodrigues, Adsorption equilibrium of methane, carbon dioxide, and nitrogen on zeolite 13X at high pressures, J. Chem. Eng. Data 49 (2004) 1095–1101.
[37] Y. Wang, M.D. LeVan, Adsorption equilibrium of carbon dioxide and water vapour on zeolites 5A and 13 X and silica gel: pure components, J. Chem. Eng. Data 54 (2009) 2839–2844.
[38] J. Zhang, P. Xiao, G. Li, P.A. Webley, Effect of flue gas impurities on CO_2 capture performance from flue gas from coal-fired power stations by vacuum swing adsorption, Energy Proc. 1 (2009) 1115–1122.
[39] B. Bonelli, B. Onida, B. Fubini, C. Otero Areán, E. Garrone, Vibrational and thermodynamic study of the adsorption of carbon dioxide on the zeolite Na-ZSM-5, Langmuir 16 (2000) 4976–4983.
[40] G. Busca, V. Lorenzelli, Infrared spectroscopic identification of species arising from reactive adsorption of carbon oxides on metal oxide surfaces, Mater. Chem. 7 (1982) 89–126.
[41] B. Bonelli, B. Civalleri, B. Fubini, P. Ugliengo, C. Otero Arean, E. Garrone, Experimental and quantum chemical studies on the adsorption of carbon dioxide on alkali-metal-exchanged ZSM-5 zeolites, J. Phys. Chem. 104 (2000) 10978–10988.
[42] T. Montanari, G. Busca, On the mechanism of adsorption and separation of CO_2 on LTA zeolites: an IR investigation, Vib. Spectrosc. 46 (2008) 45–51.
[43] G. Ramis, G. Busca, V. Lorenzelli, Low-temperature CO_2 adsorption on metal oxides: spectroscopic characterization of some weakly adsorbed species, Mater. Chem. Phys. 29 (1991) 425–435.
[44] S. Coluccia, L. Marchese, G. Martra, Characterization of microporous and mesoporous materials by the adsorption of molecular probes: FT-IR and UV-vis studies, Micropor. Mesopor. Mater. 30 (1999) 43–56.
[45] J.D. Frantz, Raman spectra of potassium carbonate and bicarbonate aqueous fluids at elevated temperatures and pressures: comparison with theoretical simulations, Chem. Geol. 152 (1998) 211–225.
[46] G. Maurin, P.L. Llewellyn, R.G. Bell, Adsorption mechanism of carbon dioxide in faujasites: grand canonical Monte Carlo simulations and microcalorimetry measurements, J. Phys. Chem. B 109 (2005) 16084–16091.
[47] A. Pulido, P. Nachtigall, A. Zukal, I. Domínguez, J. Cějka, Adsorption of CO_2 on sodium-exchanged ferrierites: the bridged CO_2 complexes formed between two extraframework cations, J. Phys. Chem. C 113 (2009) 2928–2935.
[48] E. Jaramillo, M. Chandross, Adsorption of small molecules in LTA zeolites. 1. NH_3, CO_2, and H_2O in zeolite 4A, J. Phys. Chem. B 108 (2004) 20155–20159.
[49] S. Coluccia, L. Marchese, G. Martra, Characterisation of microporous and mesoporous materials by the adsorption of molecular probes: FTIR and UV–Vis studies, Micropor. Mesopor. Mater. 30 (1999) 43–56.
[50] M. Aresta, A. Dibenedetto, E. Quaranta, Reaction Mechanisms in Carbon Dioxide Conversion, Springer, Berlin, 2016, pp. 35–70.
[51] T. Frising, P. Leflaive, Extraframework cation distributions in X and Y faujasite zeolites: a review, Micropor. Mesopor. Mater. 114 (2008) 27–63.
[52] F.F. Porcher, M. Souhassou, C.E.P. Lecomte, Experimental determination of electrostatic properties of Na–X zeolite from high resolution X-ray diffraction, Phys. Chem. Chem. Phys. 16 (2014) 12228–12236.
[53] A. Goursot, V. Vasilyev, A. Arbuznikov, Modeling of adsorption properties of zeolites: correlation with the structure, J. Phys. Chem. B 101 (1997) 6420–6428.
[54] A. Alberti, P. Davoli, G. Vezzalini, The crystal structure refinement of a natural mordenite, Z. Kristallogr. 175 (1986) 249–259.
[55] S. Devantour, A. Abdoulaye, J.C. Giuntini, F. Henn, Localization of water molecules and sodium ions in Na-mordenite, by thermally stimulated current measurement, J. Phys. Chem. B 105 (2001) 9297–9301.
[56] G. Maurin, P. Senet, S. Devantour, F. Henn, J.C. Giuntini, Modelling of the cation motions in complex system: case of Na-mordenites, J. Non-Cryst. Solids 307–310 (2002) 1050–1054.
[57] R.G. Bell, S. Devautour, F. Henn, J.C. Giuntini, Modeling the effect of hydration in zeolite Na^+-mordenite, J. Phys. Chem. B 108 (2004) 3739–3745.

[58] M. Hefti, D. Marx, L. Joss, M. Mazzotti, Adsorption equilibrium of binary mixtures of carbon dioxide and nitrogen on zeolites ZSM-% and 13X, Micropor. Mesopor. Mater. 215 (2015) 215–228.
[59] B. Vujić, A.P. Lyubartsev, Transferable force-field for modelling of CO_2, N_2, O_2 and Ar in all silica and Na^+ exchanged zeolites, Model. Simul. Mater. Sci. Eng. 24 (2016) 045002.
[60] E.P. Hunter, S.G. Lias, Proton affinity evaluation, in: P.J. Linstrom, W.G. Mallard (Eds.), NIST Chemistry WebBook, NIST Standard Reference Database Number 69, National Institute of Standards and Technology, Gaithersburg, MD, 2005 June, p. 20899 http://webbook.nist.gov.